Phase and Direction Control of a Terahertz Wave Propagating in a Waveguide Coupled With a Bull's-Eye Structure

Seigo Ohno, Yu Tokizane, Jun-ichi Shikata, and Hiroaki Minamide

Abstract – A bull's-eye structure, wherein a sub-wavelength-scale hole on a metal substrate is surrounded by a concentric circular grating structure, has been known to exhibit an anomalous transmission effect for a normal-incident electromagnetic wave when the wave resonates to the grating structure. We present a waveguide structure coupled with a bull's-eye structure introducing a simple method of symmetry breaking. In such a structure, an identical waveguide mode can be coupled with the incident light to the bull's-eye structure, even if there is a linear polarization direction while the wave experiences a phase delay through the coupling. We modeled the situation with simple formulae and numerically simulated it in a terahertz region. The results indicate the possibility of controlling the phase and the propagation direction of a terahertz wave in the waveguide via the polarization state of the incident wave to the bull's eye.

1. Introduction

Because of increasing amounts of information requiring a faster communication rate, the carrier frequency for wireless communication is expected to shift to higher frequencies. In particular, the terahertz (THz) region is attractive as a possibility for a frequency resource for rapid communication in portable devices [1]. At the first stage of signal processing, for communication within a circuit for the THz wave, phase- and direction-control techniques for a wave propagating in a waveguide play fundamental and crucial roles. In the optical region, control techniques for the waves in a waveguide have also been used for communication, and they have underpinned information in our society. Recently, propagation direction control in a waveguide has attracted attention in fundamental physics, due to its analogy with the spin–momentum-locking nature of spin–orbit interaction or the quantum spin–Hall effect in electron systems [2, 3]. In designing the controllability and functionality of the propagating wave in such a waveguide system, the near-field effect around the waveguide and the light source coupling to the waveguide play important roles.

With respect to the near-field effect, a bull's-eye structure, which consists of a concentric metallic grating with a sub-wavelength-scale hole at the center, has been found to be an artificial structure that shows anomalous transmission [4]. It works well not only in the optical region but also in the THz region [5]. The focusing nature of the incident light into the central hole of the bull's-eye structure is proposed as a sensing technique for biomolecules [6] and a high-gain antenna for capturing the propagating millimeter wave in the air [7]. As for the THz region, the coupling between the bull's-eye antenna and a waveguide have been less explored, despite proposals of many applications of THz waves; exploring coupling control is essential for realizing ultrafast THz processing devices such as THz integrated circuits using bull's-eyes.

We will focus on the bull's-eye structure's application to a THz antenna, and we assume a system that combines the bull's-eye structure with a waveguide. Here we propose phase and propagation direction control of the THz-wave propagation in such a system. The phase-control technique in the THz region has previously been reported using a liquid-crystal device [8] and a Fresnel rhomb [9]. Since these devices are bulky, they are appropriate for experiments in a laboratory but not for portable applications. In the past two decades, active metamaterials and metasurfaces have been developed as thin, lightweight devices for controlling the phase [10]. However, in many cases, due to their working principle based on resonance phenomena, the working bandwidth is restricted by the resonance bandwidth. In the optical region, an electro-optic modulator made from a nonlinear crystal, as typified by a lithium niobite crystal, is used for phase modulation and is commercially available. However, in the THz region these nonlinear materials are not practical due to the substantial absorption loss [11].

In this article, we present a simple technique for controlling the phase of the propagating wave in a waveguide introducing a simple symmetry break. It works in the broad-frequency band, meeting the

Manuscript received 27 August 2020. This work was partially supported by TOPCON CORPORATION and KAKEN (JP18K04967 and 19K05286).

Seigo Ohno is with Tohoku University, 6-3, Aramaki, Aoba-ku, Sendai 980-8578, Japan; and the RIKEN Center for Advanced Photonics (RAP), RIKEN, Aoba-ku, Sendai 980-0845, Japan; e-mail: seigo@tohoku.ac.jp.

Yu Tokizane is with the RIKEN Center for Advanced Photonics (RAP), RIKEN, Aoba-ku, Sendai 980-0845, Japan; and the Institute of Post-LED Photonics, Tokushima University, 2-1, Minami-Josanjima, Tokushima 770-8506, Japan; e-mail: yu.tokizane@riken.jp.

Jun-ichi Shikata is with the College of Engineering, Nihon University, Koriyama 963-8642, Japan; e-mail: shikata.junnichi@nihon-u.ac.jp.

Hiroaki Minamide is with the RIKEN Center for Advanced Photonics (RAP), RIKEN, Aoba-ku, Sendai 980-0845, Japan; minamide@riken.jp

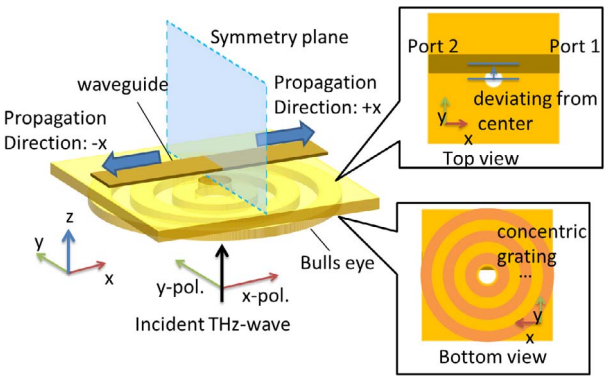

Figure 1. Configuration of the waveguide coupled with a bull's-eye. The location of the waveguide is slightly deviated from directly above the aperture in the bull's-eye.

operation frequency of an antenna structure, and is also applicable to the propagation direction-controlling technique that is analogous to spin–momentum locking. We believe this technique has the potential to be one of the fundamental techniques to support THz communication in the next generation. Since the present technique is independent of the frequency of operation, it will be widely applicable to all electromagnetic waves, ranging from microwave to optical waves, as far as antennas and waveguides are available.

2. Theory for Phase-Difference Control

We consider that a structure comprises a bull's-eye part on the front of a substrate and a waveguide part on the back, as shown in Figure 1. In this configuration, providing that a linearly polarized wave normal-incident to the bull's-eye part is focused into a center hole such that the wave passes through the hole, we consider the wave propagation in the waveguide to be dependent on the polarization direction of the incident light. The waveguide is slightly deviated from just above the hole and locates the positive y-direction. The wave coupled to the waveguide propagates while being divided between the positive and negative x-directions, and each wave reaches both ends, labeled ports 1 and 2. Note that the following discussion can work in any type of waveguide, although we assume a microstrip structure [12, 13] for the waveguide in Figure 1. Also, the lowest order mode in the waveguide is assumed in the propagation; for example, in the microstrip case, a quasi-TEM mode [12] is considered.

In the case of an x-polarized beam incidence, since the oscillation existing in the system is odd against the symmetry plane, the propagation mode should also be odd. Thus, the waves at the end ports oscillate with the opposite sign, and the phase difference between ports 1 and 2 should be out of phase.

When a y-polarized beam is incident to the bull's-eye part, the oscillation in the system becomes even. It is noteworthy that if the waveguide is located just above the hole, the lowest mode cannot be coupled with the y-polarization incident due to the geometrical symmetry, while a slight deviation of the waveguide from the center position breaks the symmetry and opens the coupling channel to the lowest order propagation mode. The waves coupled to the waveguide propagate in the $\pm x$-directions with even symmetry. Thus, at the end port of the waveguide, the phase difference between ports 1 and 2 should be zero. These can be phenomenologically formulated: for the y-polarized wave incident case,

$$|y\rangle = \begin{pmatrix} E_{\mathrm{Port1}} \\ E_{\mathrm{Port2}} \end{pmatrix} = a \begin{pmatrix} 1 \\ 1 \end{pmatrix} e^{-i\omega t} \tag{1}$$

and for the x-polarized wave incident case,

$$|x\rangle = \begin{pmatrix} E_{\mathrm{Port1}} \\ E_{\mathrm{Port2}} \end{pmatrix} = b \begin{pmatrix} 1 \\ -1 \end{pmatrix} e^{-i\omega t} \tag{2}$$

where ω denotes the frequency of the incident wave and a and b are the complex coupling coefficients for each polarization state, respectively, described as $a = Ae^{i\alpha}$ and $b = Be^{i\beta}$, with real numbers of A, B, α, and β. Since these values depend on the structural parameter, they can be tuned by optimization of the design.

Next we consider polarization in a general direction—i.e., the polarization direction is tilted by angle θ from the y-axis. The propagating waves in the $\pm x$-directions can be described with the superposition of $|x\rangle$ and $|y\rangle$ as

$$\begin{aligned} |\psi\rangle &= \sin\theta|x\rangle + \cos\theta|y\rangle \\ &= A\cos\theta \begin{pmatrix} 1 + \frac{B}{A}\tan\theta e^{i(\beta-\alpha)} \\ 1 - \frac{B}{A}\tan\theta e^{i(\beta-\alpha)} \end{pmatrix} e^{-i(\omega t-\alpha)} \end{aligned} \tag{3}$$

The phase difference ϕ between ports 1 and 2 can be derived as the argument of a complex number

$$\frac{1 + \frac{B}{A}\tan\theta e^{i(\beta-\alpha)}}{1 - \frac{B}{A}\tan\theta e^{i(\beta-\alpha)}}$$

that is easily constructible, as shown in Figure 2. The length of the blue vectors is given by $(B/A)\tan\theta$. When $(B/A)\tan\theta \to \pm\infty$, the phase difference is described as $\phi \to \pm\pi$, where $\tan\theta$ can be set to an arbitrary real number by rotating the polarization angle θ. Hence, the phase difference ϕ can also be set to an arbitrary value from $-\pi$ to $+\pi$. This shows the phase controllability in this system due to the polarization direction of the incident beam.

3. Numerical Simulations

We performed numerical experiments using a finite-difference time-domain simulation to prove our theoretical phase-control results. In our simulation, a light source was placed in the inner part of a hole to mimic the situation where a light captured by the bull's-eye part propagates into the interior of the hole, which is 100 μm in diameter. The frequency of the electromagnetic wave was set to 2 THz, which is one of the typical output frequencies of a THz emitter such as a

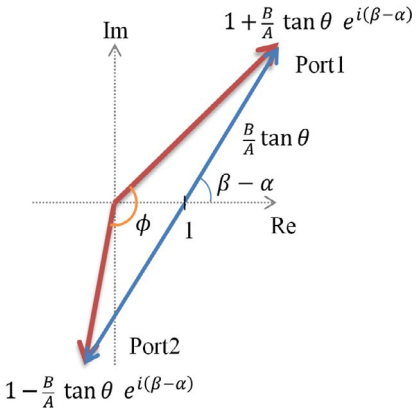

Figure 2. Drawing of phase difference ϕ on the complex plane. The length of blue vectors from (1, 0) is given as $\frac{B}{A}\tan\theta$.

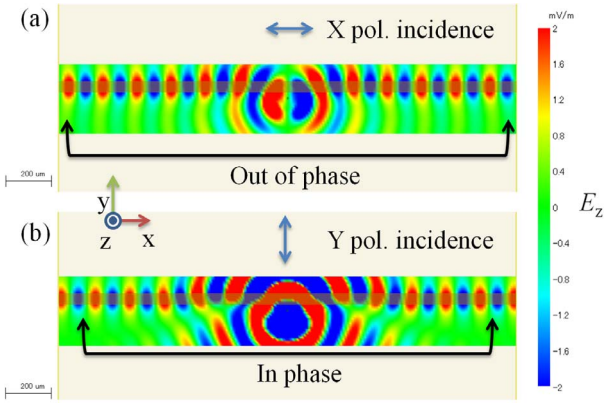

Figure 4. Distribution of z-components of the electric field within the strip line in the case of (a) x- and (b) y-polarized wave incidence. The wave at the ends of each port oscillates (a) out of and (b) in phase.

photoconductive antenna [14] or a nonlinear parametric generator using a lithium niobate crystal [15].

The waveguide part consists of a metallic substrate and a metallic ribbon located above the substrate. The ribbon width and thickness were set to 50 and 10 μm, respectively. Hereafter, this microstrip-like structure is referred to simply as a *microstrip*. The configuration and dimension of the design are shown in Figure 3. The line of the microstrip was suspended at 35 μm above a metal substrate. The wave propagated on being confined between the metallic ribbon and the metallic substrate. The center of the line was deviated 50 μm from the center of the hole to the $+y$-direction. The ends of the microstrip along the $\pm x$-directions, respectively, corresponded to ports 1 and 2. The boundary condition of the planes surrounding the simulation space was set to perfectly matching layers, to avoid unnecessary reflection at the boundaries.

The z-components of the electric field at the plane between the metallic ribbon and the substrate, under the conditions of the x- and y-polarized wave incidence cases, are shown in Figure 4a and b, respectively. In both cases, it turned out that the waves at the ends of the ports propagated with the same quasi-TEM mode, which had no node across the y-direction in the cross section of the microstrip. In the x-polarization incident case, the electric field distributed with an antisymmetric pattern against the yz-plane at the center, while in the y-polarized case, it distributed with a symmetric pattern. Comparing the phase at the end port between the polarized cases, the phase difference was found to be almost 90°. This means that there is a finite phase difference between the two polarization states when coupling to the microstrip, i.e., $\alpha \neq \beta$. Furthermore, the amplitudes at the ends are also different; thus, $A \neq B$. Consequently, according to (3) we can control the phase difference between ports 1 and 2. For instance, it was tuned to 90° by setting $E_x : E_y = 1 : 5$. The polarization angle was correspondingly set to $\theta = \arctan 1/5$. The electric distribution is shown in Figure 5a. It was found that the waves showed zero and a maximum amplitude at ports 1 and 2, respectively, meaning that the phase difference was controlled to 90°, i.e., $|\beta - \alpha| = \pi/2$. Hence, we can conclude that the phase difference between ports 1 and 2 can be controlled by the polarization angle of the incident beam.

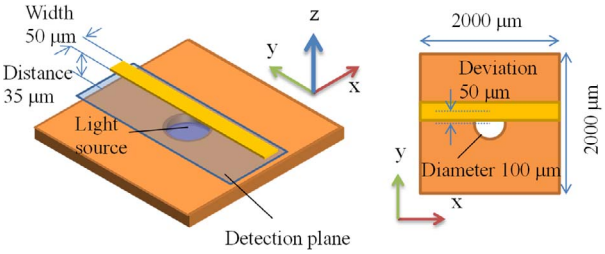

Figure 3. Structural design and dimensions of each part in the numerical simulation.

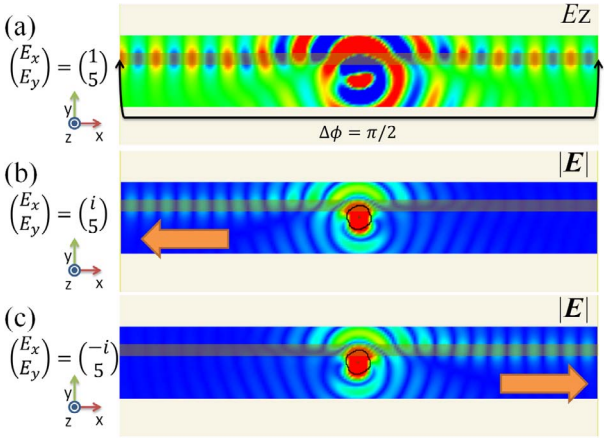

Figure 5. (a) Phase difference between ports 1 and 2 controlling to $\pi/2$. (b, c) Propagation direction controlled by handedness of elliptically polarized beam.

As an application of (3), we show the example of spin–momentum locking [2, 3]. We consider that the polarization state of the incident beam is so elliptically polarized that the phases between the x- and y-components are different, with $\pm\pi/2$ as

$$\begin{aligned}|\psi\rangle &= \sin\theta|x\rangle \pm i\cos\theta|y\rangle \\ &= A\cos\theta\begin{pmatrix} 1\pm\frac{B}{A}i\tan\theta e^{i(\beta-\alpha)} \\ 1\mp\frac{B}{A}i\tan\theta e^{i(\beta-\alpha)}\end{pmatrix}e^{-i(\omega t-\alpha)}\end{aligned} \tag{4}$$

And when $|\beta-\alpha| = \pi/2$ and $\tan\theta = B/A$, we can compute (4) as

$$\begin{aligned}|\psi\rangle &= 2A\cos\theta e^{-i(\omega t-\alpha)} \\ &= \begin{cases}\begin{pmatrix}0\\1\end{pmatrix}, & \text{when delay is } +\pi/2 \\ \begin{pmatrix}1\\0\end{pmatrix}, & \text{when delay is } -\pi/2\end{cases}\end{aligned} \tag{5}$$

This means that the propagation direction can be selected by the polarization state. Actually, when the simulation results for the polarization states are given with $E_x : E_y = \pm i : 5$, the electric-field amplitudes $|E|$ are depicted in Figure 5b and c, respectively. These figures show the switching of the propagation direction by the handedness of the elliptical polarization. The extinction ratio between the high and low signals in the intensity reached approximately 100. Such high sensitivity to the polarization state is applicable not only to the fundamental technique for THz communication but also to the basic components for measurement of the quantum state of the THz photons.

4. Conclusion

We proposed a bull's-eye structure combined with a waveguide that introduced symmetry breaking. In this system, the identical waveguide mode can be coupled with the x- and y-polarized incident lights. The phase at both ends of the waveguide depends on the polarization direction. The field distribution behaves antisymmetrically, and the symmetric features correspond to the polarization direction. When the superposed states between both polarization states were considered, it was found that the phase difference at both ends of the waveguide could be controlled by the polarization direction. This is also applicable to propagation direction switching by rotational direction of the elliptically polarized state. We believe that this phase- and direction-control technique in the THz region will allow a THz-wave manipulation technique that is usable for wireless communication, fine measurement, and quantum photonics in the THz regions.

5. References

1. K. B. Letaief, W. Chen, Y. Shi, J. Zhang, and Y.-J. A. Zhang, "The Roadmap to 6G: AI Empowered Wireless Networks," *IEEE Communications Magazine,* **57**, 8, August 2019, pp. 84-90.
2. J. Petersen, J. Volz, and A. Rauschenbeutel, "Chiral Nanophotonic Waveguide Interface Based on Spin-Orbit Interaction of Light," *Science*, **346**, 6205, October 2014, pp. 67-71.
3. M. F. Picardi, A. V. Zayats, and F. J. Rodríguez-Fortuño, "Janus and Huygens Dipoles: Near-Field Directionality Beyond Spin-Momentum Locking," *Physical Review Letters*, **120**, 11, March 2018, p. 117402.
4. J.-M. Yi, A. Cuche, E. Devaux, C. Genet, and T. W. Ebbesen, "Beaming Visible Light With a Plasmonic Aperture Antenna," *ACS Photonics*, **1**, 4, March, 2014, pp. 365-370.
5. K. Ishihara, T. Ikari, H. Minamide, J. Shikata, K. Ohashi, et al., "Terahertz Near-Field Imaging Using Enhanced Transmission through a Single Subwavelength Aperture," *Japanese Journal of Applied Physics*, **44**, 28–32, July 2005, pp. L929-L931.
6. C. R. Crick, P. Albella, H.-J. Kim, A. P. Ivanov, K.-B. Kim, et al., "Low-Noise Plasmonic Nanopore Biosensors for Single Molecule Detection at Elevated Temperatures," *ACS Photonics*, **4**, 11, September 2017, pp. 2835-2842.
7. U. Beaskoetxea, V. Pacheco-Peña, B. Orazbayev, T. Akalin, S. Maci, et al., "77-GHz High-Gain Bull's-Eye Antenna With Sinusoidal Profile," *IEEE Antennas and Wireless Propagation Letters*, **14**, September 2014, pp. 205-208.
8. A. K. Sahoo, C.-S. Yang, O. Wada, and C.-L. Pan, "Twisted Nematic Liquid Crystal Based Terahertz Phase Shifter With Crossed Indium Tin Oxide Finger Type Electrodes," *IEEE Transactions on Terahertz Science and Technology*, **9**, 4, July 2019, pp. 399-408.
9. Y. Kawada, T. Yasuda, and H. Takahashi, "Carrier Envelope Phase Shifter for Broadband Terahertz Pulses," *Optics Letters*, **41**, 5, March 2016, pp. 986-989.
10. K. Fan and W. J. Padilla, "Dynamic Electromagnetic Metamaterials," *Materials Today*, **18**, 1, January–February 2015, pp. 39-50.
11. J. Shikata, S. Ohno, and H. Minamide, "Terahertz-Wave Generation From Surface Phonons at Forbidden Frequencies of Lithium Niobate," *IEICE Electronics Express*, **17**, 11, June 2020, p. 20200133.
12. R. Garg, I. Bahl, and M. Bozzi, *Microstrip Lines and Slotlines,* 3rd ed., Boston, Artech House, 2013.
13. F. Caspers, "RF Engineering Basic Concepts: S-Parameters," CAS–CERN Accelerator School: RF for Accelerators, Ebeltoft, Denmark, June 2010, pp. 67-93.
14. J. Neu and C. A. Schmuttenmaer, "Tutorial: An Introduction to Terahertz Time Domain Spectroscopy (THz-TDS)," *Journal of Applied Physics,* **124**, 23, December 2018, p. 231101.
15. H. Minamide, "Development of High-Power Terahertz-Wave Sources for Finding Novel Applications," *IEEE Transactions on Terahertz Science and Technology*, **5**, 6, November 2015, pp. 1104-1109.